Check for updates

Original Report

Effect of Nozzle Geometry on Characteristics of Submerged Gas Jet and Bubble Noise

Journal of Laboratory Automation
2016, Vol. 21(5) 652–659
© 2015 Society for Laboratory Automation and Screening
DOI: 10.1177/2211068215584902
jala.sagepub.com
SAGE

Hai-Yan Bie[1], Jian-Jun Ye[2], and Zong-Rui Hao[3]

Abstract

Submerged exhaust noise is one of the main noise sources of underwater vehicles. The nozzle features of pipe discharging systems have a great influence on exhaust noise, especially on the noise produced by gas-liquid two-phase flow outside the nozzle. To study the influence of nozzle geometry on underwater jet noises, a theoretical study was performed on the critical weber number at which the jet flow field morphology changes. The underwater jet noise experiments of different nozzles under various working conditions were carried out. The experimental results implied that the critical weber number at which the jet flow transformed from bubbling regime to jetting regime was basically identical with the theoretical analysis. In the condition of jetting regime, the generated cavity of elliptical and triangular nozzles was smaller than that of the circular nozzle, and the middle- and high-frequency bands increased nonlinearly. The radiated noise decreased with the decrease in nozzle diameter. Combined with theoretical analysis and experimental research, three different submerged exhaust noise reduction devices were designed, and the validation tests proved that the noise reduction device with folds and diversion cone was the most effective.

Keywords

gas injection, submerged gas jet, nozzle geometry, submerged exhaust noise

Introduction

Gas injection is an integral feature of manufacturing processes, such as steelmaking, biopharming, copper converting, and aluminum refining.[1–3] The noise generated by high-velocity gas jetting into liquid is a vital concern related to the manufacturing industry. Submerged jet noise is mainly affected by the gas velocity and nozzle geometry of the underwater gas exhaust system. It is important to understand the characteristics of exhaust jet noise generated by a gas jet and the influence of exhaust outlet structures on noise level. It has been demonstrated that acoustic signals produced by bubble-bubble interaction are the major sources of submerged gas exhaust noise.[4,5] Manasseh et al.[6,7] further pointed out that noise production was influenced by bubble-size distribution and bubble interaction. From what has been discussed above, it can be concluded that the bubble transition was the main reason for the submerged gas jet noise.

Many studies have been done on the gas-liquid two-phase jet flow. Hoefele and Brimacombe[8] carried out high-speed photography and pressure measurement of gas discharging into liquid using straight and convergent-divergent nozzles. The results showed that the rate of pressure pulsation was reduced as the gas injection pressure increased and the flow transition from bubbling to jetting occurred. Linck et al.[9] described an investigation of swirl-stabilized flames created in a combustor featuring coannular swirling airflows under submerged conditions. A central atomization air jet was used to atomize methanol fuel, providing great flexibility and control over fuel spray properties in a compact geometry. Direct photography was used to examine the global features of the flame. Lin[10] showed that the discharge became less stable with an increase in density ratios. Another feature of multiphase jets involved the highly nonlinear variation of the two-phase acoustic velocity, which probably affected the gas dynamic processes for air injection into water.[11,12] Dai et al.[13]

[1]College of Chemistry and Chemical Engineering, Ocean University of China, Qingdao, China
[2]School of Power and Engineering, Huazhong University of Science and Technology, Wuhan, China
[3]Institute of Oceanographic Instrument of Shandong Academy of Science, Qingdao, China

Received Jan 27, 2015.

Corresponding Author:
Zong-Rui Hao, Institute of Oceanographic Instrument of Shandong Academy of Science, No. 28, Zhejiang Road, Qingdao, Shandong, China, Qingdao, 266001, China.
Email: positivesss@163.com

conducted experiments to analyze the flow pattern and hydrodynamic effect of underwater gaseous jets from sonic and supersonic nozzles. The results showed that a high-speed gas jet into stagnant water could induce large pressure pulsations in the upstream of the nozzle exit and that the shock-cell structures in the over- and underexpanded jets could lead to a strong hydrodynamic pressure.

The noise of gas jets and the acoustic characteristics of bubbles have been studied for many decades.[14] Xu et al.[15] studied the acoustic emission characteristics of underwater gas jets experimentally. It was revealed that increasing gas velocity elongated and strengthened the bubbles and increased acoustic emission. Gavigan et al.[16] measured the noise radiated by gas exhausting into a turbulent wake under controlled conditions. The results showed that radiated noise was affected by the orifice size, flow rates, and critical weber number. Vazquez et al.[17] pointed out that chaos could appear in the bubble size and bubble production rate independently. The radiated sound from the turbulent underwater gas jet under different flow rates and orifice sizes was investigated by Chen et al.[18] They revealed that orifice size played an important role in the generation of noise. But when the discharge velocity was greater than the critical value, the noise was independent of the orifice size. Wilson et al.[19] analyzed circular, elliptical (aspect ratio of 3:1), and rectangular (aspect ratio 3:1) nozzles for heated gas injection in water. It was revealed that the spread at the major axis plane for the elliptical nozzle was similar to the circular nozzle. The jets were found to penetrate more into the water, and better mixing was observed as compared with jets from circular nozzles. Arghode et al.[20] found that sound pressure levels for elliptical nozzles were lower than those of circular, square, and triangular nozzles. However, the radiated noise induced by a submerged gas jet was monitored in air, and the sound pressure levels were limited from 10 Hz to 1 kHz. Sound levels greater than 1 kHz were not considered.

In the present work, five underwater nozzles with different structures were designed to explore the most optimum method for noise reduction. The effects of the nozzle structures and gas velocity on the sound pressure levels in the frequency bands of 0.6 to 10 kHz were investigated by experimental measurements. Then underwater jet noise experiments with circular nozzles were conducted with the same weber number. Finally, three different submerged exhaust noise reduction devices were designed according to the theoretical analysis and experimental research, and validation tests were carried out to investigate noise reduction effects of the designed noise reduction devices.

Critical Weber Number

The gas-liquid two-phase flow is produced when gas is injected into liquid. With the increase in gas rate, the two-phase flow regime will transform from bubbling regime to jetting regime. At low velocity, the bubble interface is smooth, and the flow is in bubbling flow. If the velocity is high enough, which occurs when the weber number is larger than the critical weber number, rippling of the bubble surface occurs. The mixture of gas and liquid droplets can then push deeply into the liquid, many small bubbles arise, and the flow is in jetting flow.

The first bubble formed at the orifice in the beginning of underwater exhaust is taken to study the critical weber number at which the jet flow field morphology changes. According to the studies by Kitscha and Kocamustafaogullari[21] and Zhao and Irons,[22] when air is injected into water, the growth factor k_c of the disturbance can be obtained by the following equation:

$$kc = \left(\rho^* U_a{}^2 k^2 - \frac{\sigma k^3}{\rho_w} + gk \right)^{1/2}, \tag{1}$$

where ρ^* is the gas-to-liquid density ratio, U_a is the gas velocity, g is the acceleration of gravity, k is the wave number, ρ_w is the density of water, and σ is the surface tension.

The most affected wavelength is the one with the maximum growth factor. It can be calculated by differentiating eq 1 with respect to k and setting the derivative to zero. Then, the wave number k is obtained as

$$k = \frac{\rho^* \rho_w U_a{}^2 \pm \sqrt{\rho^{*2} \rho_w{}^2 U_a{}^4 + 3\sigma g \rho_w}}{3\sigma}. \tag{2}$$

The magnitude of the second term in the square root in eq 2 is always substantially smaller than the first term, so it can be neglected. As a consequence, the critical wave number is simplified as

$$k = \frac{2\rho_a U_a{}^2}{3\sigma} = \frac{2We}{3d_o}, \tag{3}$$

where ρ_a is the density of the air, We is the weber number, $We = \frac{\rho_a U_a{}^2 d_o}{\sigma}$, and d_o is the diameter of the nozzle. Substituting k into eq 1, the maximum growth factor is expressed to be

$$kc = \sqrt{\frac{4\sigma We^3}{27\rho_w d_o{}^3}}. \tag{4}$$

The growth time and the propagation time can be expressed by the following equations[23]:

$$t_g = \frac{C_g}{kc}. \tag{5}$$

$$t_p = 0.25\frac{d_o}{U_a}. \tag{6}$$

Table 1. Underwater Exhaust Noise Experiment Parameters of the Nozzles of Different Structures.

Case	Gas Velocity (m/s)	Gas Flow Rate (L/s)	Reynolds Number	Weber Number
1	35	2.08	20,384	176
2	42	2.5	24,460	254
3	49	2.92	28,537	345
4	56	3.33	32,614	451

If the propagation time is greater than the growth time, the interface will break up, and the flow regime transforms from the bubbling to jetting regime. The following relation is obtained:

$$0.25\frac{d_o}{U_a}\sqrt{\frac{4\sigma We^3}{27\rho_w {d_o}^3}} \geq C_g. \quad (7)$$

If C_g is 1, the critical weber number can be yielded to be

$$W_e = \frac{10.39}{\sqrt{\rho^*}}. \quad (8)$$

The subject studied in this article is an air-water injection system; hence, the critical weber number is about 288.

Setup of Experiments on Submerged Exhaust Noise

To study the submerged exhaust noise spectrum characteristics formed upon different structures of nozzles, an optically accessible experimental test section was developed and constructed. The water tank was made with Plexiglass and was 0.45 m id, 0.8 m high. The nozzle at the center of the tank bottom was immersed into water with a height of 450 mm. The pressure was measured with a pressure transducer, and the gas velocity was measured with an SBL (Ultra-short Baseline Positioning System)-type display target flow gauge.

The sound signals emitted from the underwater gas jet were collected by an RHS-30 standard hydrophone. Its working frequency range was 20 Hz to 50 kHz, the horizontal directivity was ±1.5 dB (50 kHz), the vertical directivity was ±2.0 dB (50 kHz), and the low-frequency receiving sensitivity was −193 dB. The hydrophone should be placed as closely as possible to the sound source to ensure that the received sound signals radiate from the underwater gas jet noise. In this experiment, the RHS-30 standard hydrophone was positioned about 150 mm above the nozzle outlet and 200 mm away from the water tank at the same plane of outlet nozzle. The signals were recorded simultaneously by a four-channel digital storage oscilloscope (TDS2000) digitizing at 51.2 kHz.

Five underwater nozzles with different structures were designed to investigate the characteristics of exhaust jet under different jet momentums: the round nozzle, the rectangular nozzle, the triangular nozzle, and two elliptical nozzles with aspect ratios of 1.5 and 2.5. All five nozzles were of the same cross-sectional area with the circular nozzle of 8.7 mm. The corresponding experiment parameters are listed in **Table 1**.

To study the influence of nozzle diameter on jet noise, four circular nozzles with different diameters of 4, 6, 8.7, and 10 mm were designed. The corresponding experiment parameters are listed in **Tables 2 and 3**. For the minimum flow rate in all experiments, the Reynolds number reached 20,384, which was higher than 4000. Therefore, all the outlet gas flow was turbulent. In addition, all experiments were carried out at the room temperature of 300 °K and water temperature of 298 °K.

Analysis of the Flow Field Form

Transformation of the Flow Field Form

Images of the exhaust jets produced by the circular nozzle of 8.7 mm at different gas flow rates are shown in **Figure 1**. When the gas flow rate was very low, the bubbles formed at the nozzles were governed by a force balance between surface tension buoyancy forces. The bubbles along the jet axis were spherical. With the expansion and forward movement of the bubble, pressure of the bubble tail decreased gradually. The bottom of the bubble transformed from expansion to contraction, and new bubbles formed. It can be seen from **Figure 1a** that the bubble interface appeared smooth. However, with the increase of gas velocity, rippling of the bubble surface occurred, as shown in **Figure 1b**. If the gas velocity was high enough, the ripples would not be damped, the interface broke up, droplets of liquid entrained into the gas, and smaller bubbles were produced, which indicated the transition from the bubbling regime to the jetting regime, as shown in **Figure 1c**. When the weber number exceeded the critical weber number, the shedding rates of bubbles were greatly accelerated. As the turbulence intensity of the submerged gas jet increased, many small bubbles presented, as can be seen in **Figure 1d**. In addition, a "cavity" can be observed surrounding the nozzle, which lessened with the increase of gas flow rates.

Sound Pressure Signals

The pressure signals of the gas-liquid flow field were significantly affected by the transition flow field form from the

Table 2. Underwater Exhaust Noise Experiment Parameters of the Circular Nozzles.

Gas Volume Flow(L/s)	Diameter (mm)	Gas Velocity (m/s)	Reynolds Number (*Re*)	Weber Number (*We*)
2.08	4	165	44,336	1816
	6	74	29,557	538
	8.7	35	20,384	176
	10	26	17,734	116
2.5	4	199	53,203	2615
	6	88	35,469	775
	8.7	42	24,460	254
	10	32	21,281	167
2.92	4	231	62,071	3560
	6	103	41,380	1054
	8.7	49	28,537	345
	10	37	24,828	228
3.33	4	265	70,938	4649
	6	118	47,292	1377
	8.7	56	32,614	451
	10	42	28,375	301

Table 3. Underwater Exhaust Noise Experiment Parameters of the Circular Nozzles under the Same Weber Number.

Weber Number (*We*)	Diameter (mm)	Gas Volume Flow (L/s)	Reynolds Number (*Re*)	Gas Velocity (m/s)
538	6	2.08	29,557	74
	8.7	3.63	35,867	61
	10	4.47	38,150	57

bubbling regime to the jetting regime. The sound pressure signals obtained from the circular nozzle under different flow patterns are shown in **Figure 2**. It is known that shedding, fragmentation, and coalescence of the bubbles are the major sources of noise in the bubbling regime. The corresponding pressure signals were periodic and exhibited damped sinusoidal oscillation, as shown in **Figure 2a**. With the increase in the gas flow rates, the regular and order bubbling regime became unstable. The flow field was gradually changed from a bubbling regime to jetting regime. It can be seen from **Figure 2b** that the sound pressure signals became irregular and the fluctuation in amplitude increased. With even further increases in flow rate, the flow field was transformed into a jetting regime, and the sound pressure signals presented irregular and aperiodic and were modulated by low-amplitude and high-frequency fluctuation, as shown in **Figure 2c**.

Sound Spectrum Analysis

Effects of Nozzle Structures on the Sound Spectrum

The sound spectra associated with the circular nozzle of 8.7 mm under various conditions are shown in **Figure 3**. The condition parameters corresponding to the experiment parameters are as listed in **Table 1**. As can be seen, there were obvious variations in sound pressure amplitude in the frequency bands of 0.6 to 10 kHz at different weber numbers. When the weber number was less than the critical value, the influence of weber number on the sound pressure levels was smaller. When the weber number increased to 345, the flow field was transformed from bubbling regime to jetting regime. The sound pressure level increased significantly, especially in the frequency bands of 0.6 to 4 kHz. One probable reason was that the transformation of the flow from bubbling regime to jetting regime resulted in a greater increase of turbulence intensity and a decrease of the maximum bubble volume in the flow field. The fragmentation and coalescence process among the bubbles became more and more intense; hence, the acoustic signals that radiated from the interaction between the bubbles were strengthened. The results also revealed that the sensitive spectrum of underwater jet noise was 0.6 to 10 kHz.

Figure 4 showed the sound pressure levels generated by all of the nozzles. At very low gas flow rates, the generation of the broadband sound levels was primarily attributed to the shedding of bubbles from the nozzle and to the fragmentation downstream. It can be seen from **Figure 4a** that the sound pressure levels generated by all the nozzles except

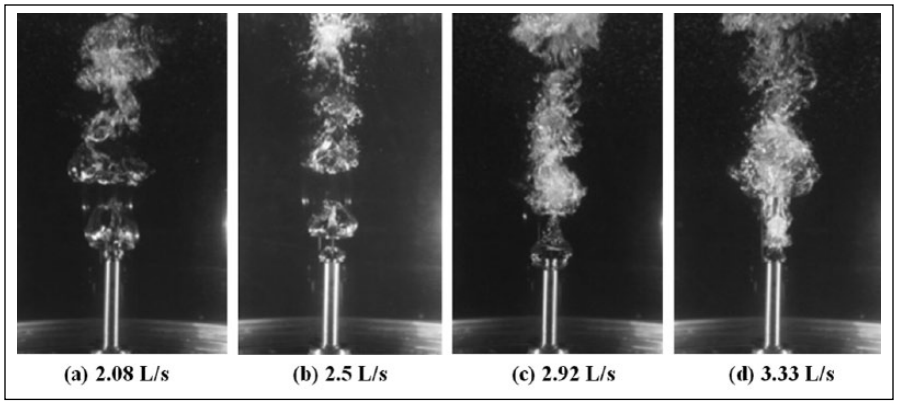


Figure 1. Exhaust jets at different weber numbers for the circular nozzle.

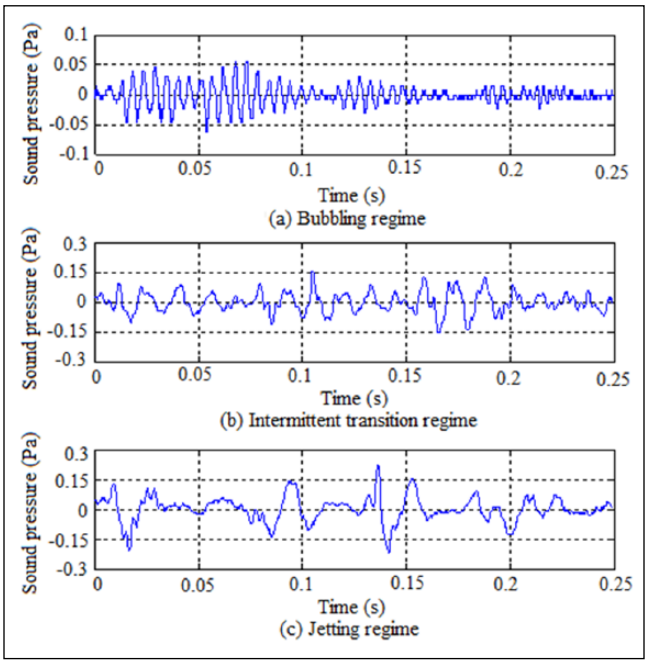


Figure 2. Sound pressure signals in different flow regimes.

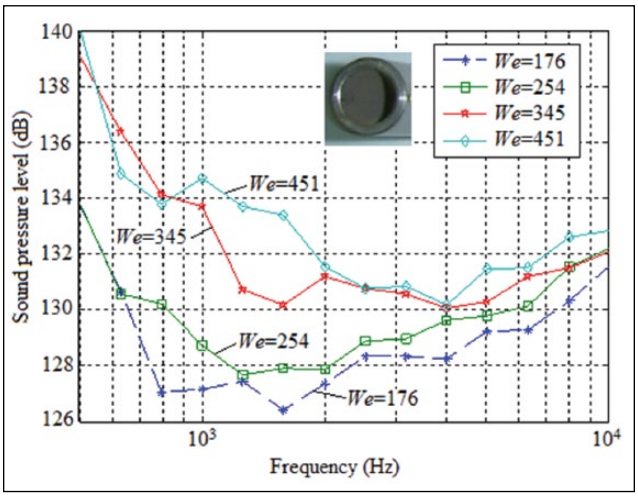


Figure 3. Sound spectra associated with the circular nozzle.

the triangular nozzle were almost the same. It seems that the influence of bubble shape on the sound pressure signal was small. The reason for the difference of sound pressure levels between the triangular nozzle and the other nozzles was considered to be the nonaxisymmetric structure of the cross section.

The turbulent intensity and bubble-bubble interaction were much more violent in the jetting regime than those in bubbling regime. Thus, the radiated acoustic signals had significant differences in the two regimes. It can be seen from **Figure 5b** that the sound pressure levels generated by the elliptical nozzle with an aspect ratio of 2.5 in the frequency bands of 0.6 to 10 kHz were the lowest. The sound pressure levels of the rectangular nozzle and triangular nozzle were higher than those of the other nozzles, whereas the highest sound pressure was generated by the rectangular nozzle. At 0.63 kHz, the sound pressure of the rectangular nozzle was 11 dB higher than that of the elliptical nozzle with an aspect ratio of 2.5. The sound pressure of the triangular nozzle was lower than that of the circular nozzle but higher than that of the elliptical nozzle with an aspect ratio of 1.5.

Comparison of **Figure 4a and b** showed that the acoustic emissions over the frequency bands of 0.6 to 4 kHz for circular, rectangular, and triangular nozzles had significant increases after the transition from a bubbling regime to jetting regime. The sound pressure level for the elliptical nozzle was much lower than those of the circular, rectangular, and triangular nozzles in the jetting regime. It had been mentioned above that the mean velocity and gas momentum at the outlet of nozzles were identical in the experiments. But because of the variation of the structure of nozzle cross sections, the interaction between the gas and water at the outlets of nozzles was different. Gas flow jetted from the elliptical nozzle with aspect ratio of 2.5 can entrain more environmental liquid than those jetted from other nozzles.

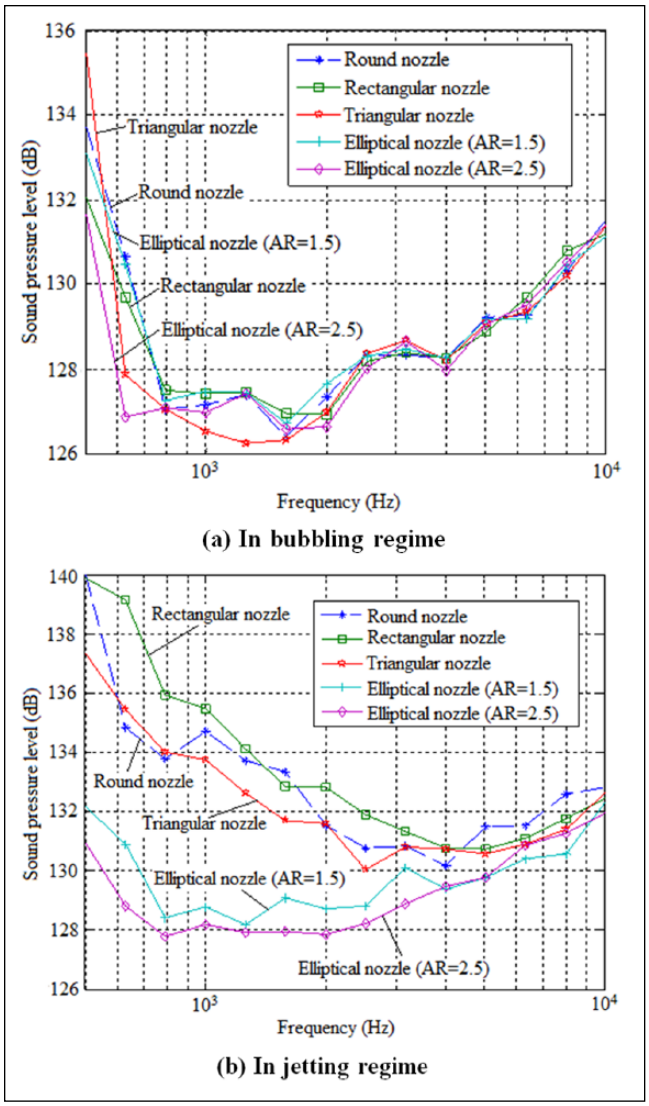


Figure 4. Sound pressure level generated by all the nozzles.

The entrained liquid by gas jetting produced a mixed gas-liquid flow, which effectively prevented the emergence of large bubbles at the outlet of the nozzle. Therefore, the great excitation produced by the shedding of large bubbles and the interaction between bubbles downstream was avoided. As a result, the noise radiated by submerged gas exhaust was greatly weakened.

When the frequency was greater than 4 kHz, the sound pressure spectra of all the nozzles were identical. Hence, it can be concluded that a suitable cross section of the nozzle can effectively reduce the noise generated by a submerged gas jet in the frequency band of 0.6 to 4 kHz but had little effect on the sound pressure above 4 kHz. Above all, the elliptical nozzle (AR = 2.5) was the optimal structure to control the sound pressure level.

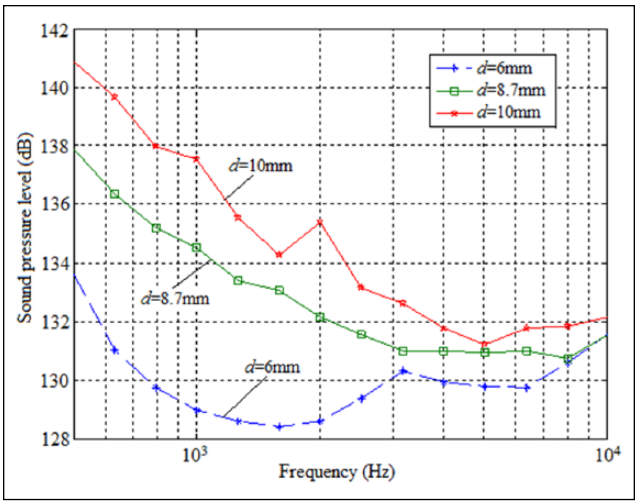


Figure 5. Sound spectra associated with the circular nozzles at *We* = 538.

Effects of Nozzle Diameters on the Sound Spectrum

Figure 5 shows the sound spectra associated with the circular nozzles at *We* = 538. According to the section of Critical Weber Number, the flow forms were all jetting regimes under the experimental conditions. It can be seen that the sound pressure level generated by the underwater gas jet at the same weber number increased with the increase in nozzle diameter. Thus, when the ratio of the gas flow rates and the surface tension was the same, the smaller the nozzle diameter, the smaller the radiated noise. As a consequence, it would be better to adopt a small-diameter nozzle instead of a large-diameter nozzle or to use a small nozzle array instead of one large-diameter nozzle with the same flow area.

Study of Submerged Exhaust Noise Reduction Devices

Design of Submerged Exhaust Noise Reduction Devices

According to the studies above, it can be included that the underwater exhaust sound pressure level was greatly affected by the structure and diameter of the nozzles and that the elliptical and small nozzle can effectively reduce the underwater noise produced by an underwater gas jet. Based on this, we designed three types of submerged exhaust noise reduction devices, as shown in **Figure 6**.

Figure 6a shows the noise reduction device with folds and diversion cone (hereinafter referred to as 1#). The elliptic fold structure was used around the wall of the device, and a droplet-type multihole cone director structure was

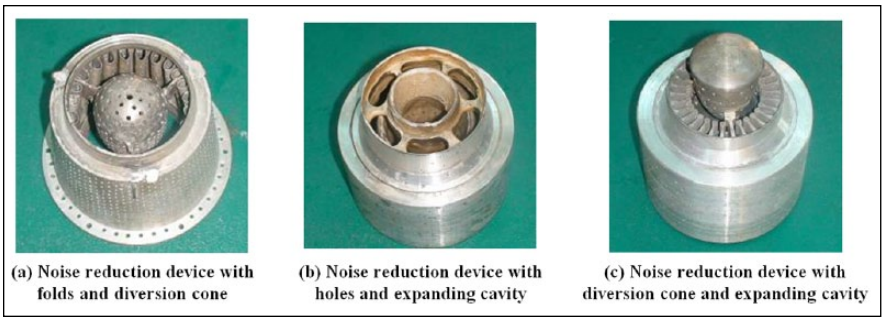


Figure 6. Designed noise reduction devices.

arranged along the axisymmetric line in the end cavity. When the high-speed exhaust gas entered into the cavity through the exhaust pipe, the jet was dispersed because of the cone director structure, and the length of the high-speed core region decreased. In addition, part of the gas flow would be shunted by the elliptic fold structure around the wall, then mixed with the surrounding liquid, and discharged through the small holes in the wall. Thus, a large number of tiny bubbles was produced instead of a large volume of bubbles.

The noise reduction device shown in **Figure 6b** constituted holes and expanding cavity (hereinafter referred to as 2#). The traditional small-hole muffler structure of high-pressure exhaust in the air was imported. Several elliptical holes were set at the end of the cross section of the cavity with relatively large spacing, arranged in circular distribution. In the front of the orifice plate, cylindrical diffusion chambers were adopted. When the exhaust gas entered into the cavity, it would expand in the cylindrical diffusion chambers and interact with the surrounding liquid, finally jetting into the water with plenty of small bubbles.

Figure 6c illustrates the noise reduction device with diversion cone and expanding cavity (hereinafter referred to as 3#). It was designed by combining the noise reduction devices of 1# and 2#. There was a director structure with a blunt edge along the axisymmetric line. The exhaust gas was shunted by the director structure and entered the diffusion chambers, finally discharging into the water through the flat slits.

Effect of Validation of Designed Submerged Exhaust Noise Reduction Devices

Submerged exhaust noise experiments under specified conditions were conducted to verify the effects of the three types of noise reduction devices. The experimental results are shown in **Figure 7**. It can be seen that the sound pressure levels decreased in the frequency bands of 1 kHz to 10 kHz after the noise reduction devices were employed. The effect of 2# was not as good as the other two; a great peak of sound pressure appeared at 2 kHz. One possible reason for this was that the

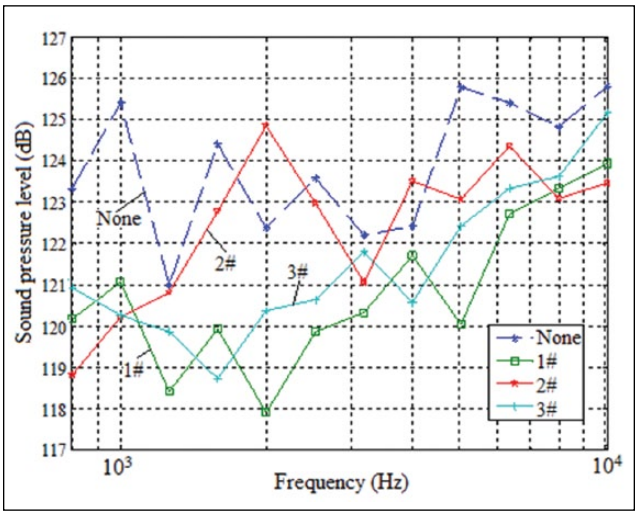


Figure 7. Effects analysis of the noise reduction devices.

gas flow expanded rapidly to form a large volume of bubbles in the cavity of 2#. The shape and volume of the bubble changed constantly and caused strong vibration. Among the three noise reduction devices, the overall noise reduction effect of 1# was the best, and the bubble noise in the frequency bands of 1 kHz to 5 kHz was controlled effectively. From **Figure 7**, it can be seen that the sound pressure level was decreased by 3 to 7 dB after using the 1# noise reduction device. The noise reduction effect of 3# was not as good as that of 1# but was better than that of 2#.

The experimental results indicated that the structure with holes and expanding cavity could not reduce submerged exhaust noise alone. When introducing the diversion cone, the exhaust gas flow was diverted by the diversion cone and mixed with the surrounding water, resulting in a reduction in exhaust noise. If we improve the expanding cavity into the elliptic fold structure, part of the exhaust gas flow is first shunted into a small gas flow and jetted into the water through the elliptic pipe in small bubble form. The other gas flow discharged into water through the diversion cone. Because the gas flow was disturbed severely by the inner surface of the elliptic fold structure, the exhaust gas was

mixed with the fluid within the cavity and formed a large number of small bubbles. This indicated that the 1# noise reduction device enhanced the mixing of gas and liquid obviously and that the volume of the generated bubbles was limited. Therefore, the submerged exhaust noise was induced effectively.

Conclusions

Five types of nozzles with the same cross-section area were designed and experimentally studied under several conditions. The results implied that the elliptical nozzle (AR = 2.5) was the optimal structure to control the sound pressure level, and the smaller the nozzle diameter, the smaller the radiated noise. Combining with theoretical analysis and experimental research, three different submerged exhaust noise reduction devices were designed, and the validation tests proved that the noise reduction device with folds and diversion cone was the most effective.

Declaration of Conflicting Interests

The authors declared no potential conflicts of interest with respect to the research, authorship, and/or publication of this article.

Funding

The authors disclosed receipt of the following financial support for the research, authorship, and/or publication of this article: This research is funded by the National Natural Science Foundation of China (No. 51106137, 51206101, and 51306166).

References

1. Koh, S. R.; Meinke, M.; Schröder, W. Impact of Multi-Species Gas Injection on Trailing-Edge Noise. *Comput. Fluids* **2013**, *75*, 72–85.
2. Ceccio, S. L. Friction Drag Reduction of External Flows with Bubble and Gas Injection. *Annu. Rev. Fluid Mech*. **2010**, *42*, 183–203.
3. Shao, P.; Zhang, T.; Zhang, Z.; et al. Numerical Simulation on Gas-Liquid Flow in Mechanical-Gas Injection Coupled Stirred System. *ISIJ Int*. **2014**, *54*, 1507–1516.
4. Chicharro, R.; Vazquez, A. The Acoustic Signature of Gas Bubbles Generated in a Liquid Cross-Flow. *Exp. Therm. Fluid Sci*. **2014**, *55*, 221–227.
5. Leighton, T. G.; Walton, A. J. An Experimental Study of the Sound Emitted from Gas Bubbles in a Liquid. *J. Phys*. **1987**, *8*, 98–104.
6. Manasseh, R.; Nikolovska, A.; Ooi, A.; et al. Anisotropy in the Sound Field Generated by a Bubble Chain. *J. Sound Vib*. **2004**, *278*, 807–823.
7. Manasseh, R.; Zhu, Y. G. Passive Acoustic Bubble Sizing in Sparged Systems. *Exp. Fluids* **2001**, *30*, 672–682.
8. Hoefele, E. O.; Brimacombe, J. K. Flow Regimes in Submerged Gas Injection. *Metall. Trans*. **1979**, *10*, 631–648.
9. Linck, M.; Gupta, A. K.; Yu, K. Submerged Combustion and Two-Phase Exhaust Jet Instabilities. *J. Propul. Power* **2009**, *25*, 522–532.
10. Lin, M. C. Transient Gas Jets in Liquids. Ph.D. Thesis, California Institute of Technology, 1986.
11. Semanov, N. I.; Kosterin, S. I. Results of Studying the Speed of Sound in Moving Gas-Liquid Systems. *Teloenergetika* **1964**, 11–46.
12. Wallis, G. B. One-Dimensional Two-Phase Flow. McGraw-Hill, New York, 1969.
13. Dai, Z. Q.; Wang, B. Y.; Qi, L. X.; et al. Experimental Study on Hydrodynamic Behaviors of High-Speed Gas Jet in Still Water. *Acta Mech. Sin*. **2006**, *22*, 443–448.
14. Rayleigh, L. On the Pressure Developed in a Liquid during the Collapse of a Spherical Cavity. *Philos. Mag*. **1917**, *34*, 4–98.
15. Xu, W. W.; Lai, Z. N.; Wu, D. Z.; et al. Acoustic Emission Characteristics of Underwater Gas Jet from a Horizontal Exhaust Nozzle. *Appl. Acoust*. **2013**, *74*, 845–849.
16. Gavigan, J. J.; Watson, E. E.; King, W.F. III. Noise Generation by Gas Jets in a Turbulent Wake. *J. Acoust. Soc. Am*. **1974**, *56*, 1094–1099.
17. Vazquez, A.; Manasseh, R.; Sanchez, R. M. Experimental Comparison between Acoustic and Pressure Signals from a Bubbling Flow. *Chem. Eng. Sci*. **2008**, *63*, 5860–5869.
18. Chen, L.; Manasseh, R.; Nikolovska, A. Noise Generation by an Underwater Gas Jet. Proc. 8th Western Pacific Acoustics Conference, Melbourne, Australia, 2003.
19. Wilson, K. J.; Gutmark, E.; Schadow, K. C.; et al. Supersonic Submerged Heated Jets. In: 28th Joint Propulsion Conference and Exhibit, Nashville, TN, 1992, Paper No. AIAA-92-3138.
20. Arghode1, V. K.; Gupta, A. K.; Yu, K. H. Effect of Nozzle Exit Geometry on Submerged Jet Characteristics in Underwater Propulsion. Proc. 46th AIAA Aerospace Sciences Meeting and Exhibit, Reno, NV, 2008.
21. Kitscha, J.; Kocamustafaogullari, G. Breakup Criteria for Fluid Particles. *Int. J Multiphas. Flow* **1989**, *15*, 573–588.
22. Zhao, Y. F.; Irons, G. A. The Breakup of Bubbles into Jets during Submerged Gas Injection. *Metall. Mater. Trans. B* **1990**, *21*, 997–1003.
23. Clift, R.; Grace, J. R.; Weber, M. E. *Bubbles, Drops and Particles*; Academic Press, New York, 1978.